Photodecomposition of dyes on Fe-C-TiO$_2$ photocatalysts under UV radiation supported by photo-Fenton process

B. Tryba [a,*], M. Piszcz [a], B. Grzmil [a], A. Pattek-Janczyk [b], A.W. Morawski [a]

[a] Szczecin University of Technology, ul. Pulaskiego 10, 70-322 Szczecin, Poland
[b] Jagiellonian University, ul. Ingardena 3, 30-060 Krakow, Poland

ABSTRACT

Fe-C-TiO$_2$ photocatalysts were prepared by mechanical mixing of commercial anatase TiO$_2$ precursor with FeC$_2$O$_4$ and heating at 500–800 °C under argon flow. These photocatalysts were tested for dyes decomposition: Methylene Blue (MB), Reactive Black (RB) and Acid Red (AR). The preliminary adsorption of dyes on the photocatalysts surface was performed. Modification of anatase by FeC$_2$O$_4$ caused reducing of zeta potential of the photocatalyst surface from +12 to −7 mV and decreasing of their adsorption ability towards RB and AR, which were negatively charged, −46.8 and −39.7, respectively. Therefore, unmodified TiO$_2$ showed the highest degree of RB and AR decompositions in the combination of dyes adsorption and UV irradiation. Methylene Blue, which had zeta potential of +4.3 in the aqueous solution was poorly adsorbed on all the tested photocatalysts and also slowly decomposed under UV irradiation. The high rate of dyes decomposition was noted on Fe-C-TiO$_2$ photocatalysts under UV irradiation with addition of H$_2$O$_2$. It was observed, that at lower temperatures of heat treatment such as 500 °C higher content of carbon is remained in the sample, blocking the built in of iron into the TiO$_2$ lattice. This iron is reactive in the photo-Fenton process resulting in high production of OH radicals and also high activity of the photocatalyst. At higher temperatures of heat treatment, less active FeTiO$_3$ phase is formed, therefore Fe-C-TiO$_2$ sample prepared at 800 °C showed low photocatalytic activity for dyes decomposition. Fe-C-TiO$_2$ photocatalysts are active under visible light irradiation, however, the efficiency of a dye decomposition is lower than under UV light. In a dark Fenton process there is observed an insignificant generation of OH radicals and very little decomposition of a dye, what suggests the powerful of photo-Fenton process in the dyes decomposition.

© 2008 Elsevier B.V. All rights reserved.

1. Introduction

Industrial dyestuffs including textile dyes are recognized as being an important environmental threat. Physical, chemical, and biological methods are available for treatment of such waste, however, they are not sufficient and advantageous, therefore applying advanced oxidation processes (AOPs) seems to be reasonable. AOPs are attractive in providing a promising and competitive solution for the abatement of numerous hazardous compounds in wastewater including Fenton or photo-assisted Fenton process, ozone or/and peroxide photolysis, and semiconductor photocatalysis process. Generated in AOPs hydroxyl radicals drive an oxidation processes, which are suitable for achieving the complete elimination and mineralisation of various pollutants such as phenols, chlorophenols, pesticides, alcohols, azo dyes, pharmaceutics, humic acids, organic acids and others [1–6].

Both, photocatalysis and photo-Fenton reactions can give rise of OH radicals formation, which have been known as the strong and no selective oxidisers of the organic matter in water. Iron is the most commonly used metal as a Fenton reagent and can be used in the form of iron salt as a homgeneous catalyst or as a heterogeneous catalyst in the form of a supported metal. The latter one is being more advantageous, because can be reused in the following processes. In photo-Fenton process OH radicals are produced in the following reactions [1]:

$$Fe^{2+} + H_2O_2 \rightarrow Fe^{3+} + HO^\bullet + HO^- \qquad (1)$$

$$Fe^{3+} + HO^- + h\nu \rightarrow Fe^{2+} + HO^\bullet \qquad (2)$$
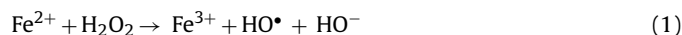
The reaction (1) proceeds much faster than reaction (2), thus the yield of photo-Fenton reactions is higher in the excess of the Fe^{2+} ions. Reduction of Fe^{3+} ions occurs in the presence of UV light.

Doping of iron to TiO$_2$ has been widely described by the others, because iron doping can give some benefits such as retarding the inconvenient recombination reaction, which proceeds after photocatalyst excitation and also can extend the photocatalytic

ability of the photocatalyst to the visible region [7–10]. However, it was proved that the photoactivity of Fe/TiO$_2$ catalyst depended on the way of preparation that influenced the amount and state of iron [11–14].

Different methods of Fe/TiO$_2$ preparation have been reported [11–14], such as impregnation of TiO$_2$ with aqueous solution of Fe(NO$_3$)$_3$·9H$_2$O or sol–gel method from TiCl$_4$ and Fe(NO$_3$)$_3$·9H$_2$O precursors. It has been reported that Fe/TiO$_2$ prepared by the sol–gel method was less active than TiO$_2$ due to the fact that dopants acted rather as recombination centers than a trap sites for charge transfer. Thus, the obtained photocatalysts revealed the lower amount of surface hydroxyl groups and a lower anatase-to-rutile ratio compared to TiO$_2$ precursor sample. The extent of doping is also important, because the presence of separated hematite or pseudobrookite (Fe$_2$TiO$_5$) phases in samples containing more than 2% of iron can decrease the catalyst activity [11]. It has been also proved that the excess of deposited iron on TiO$_2$ can form Fe(OH)$^{2+}$ species, which has the greater adsorption to the incidence light in the range of 290–400 nm than TiO$_2$, and can decrease the Fe/TiO$_2$ photoactivity [14]. The low temperature of calcination, such as 300 °C in Fe/TiO$_2$ preparation appeared to be favored taking into account its photoactivity [14].

Hematite can work as a photocatalyst and can decompose some organic compounds, like aniline or benzo[*a*]pyren [15,16]. However, the mixture of Fe$_2$O$_3$ and TiO$_2$ has been reported to be less active than original TiO$_2$ itself [17,18].

Recently, we have developed a new group of Fe-C-TiO$_2$ photocatalysts. It was reported [19–22] that Fe-C-TiO$_2$ photocatalyst could work in photo-Fenton process in water purification under UV irradiation and hydrogen peroxide addition. The prepared Fe-C-TiO$_2$ photocatalysts contained both forms of iron, Fe(II) and Fe(III), but these samples with low content of carbon contained more iron in the form of Fe(III). Sample prepared at 500 °C showed higher photoactivity under UV irradiation with H$_2$O$_2$ than the other samples heated at higher temperatures such as 600–900 °C [21]. In this paper the photoactivity of Fe-C-TiO photocatalysts towards dyes decomposition is discussed in relation to dyes adsorption on the photocatalyst surface, zeta potential of the photocatalysts and reactivity of iron phases in photo-Fenton process.

2. Experimental

2.1. Photocatalyst preparation

Commercially available anatase structure TiO$_2$ precursor obtained from the Chemical Factory Police S.A. in Poland has been used for preparation. Anatase type TiO$_2$ contained a small amount, about 3.5 wt% of rutile, and exhibited high BET surface area, around 300 m^2/g. Fe-C-TiO$_2$ photocatalysts were prepared from powders of TiO$_2$ and FeC$_2$O$_4$, detailed preparation was described elsewhere [22].

2.2. Characterization of Fe-C-TiO$_2$ photocatalyst

The phase composition and the crystal structure of Fe-C-TiO$_2$ samples were characterized by XRD powder diffraction and Mössbauer spectroscopy techniques. XRD measurements were performed in X'Pert PRO diffractometer of Philips Company, with CuKα lamp (35 kW, 30 mA). Obtained XRD patterns were compared with JCPDS (Joint Committee on Powder Diffraction Standards) cards. The Mössbauer spectra were recorded at room temperature by means of conventional spectrometer in transmission geometry using ^{57}Co in a Rh matrix. The samples were prepared in pellets with a thickness of ca. 10 mg Fe/cm^2. The spectra were numerically analyzed by the least-squares procedure assuming Lorentzian

line shapes. Isomer shifts are quoted relative to α-Fe. The respective amounts of various phases present in the samples were determined assuming equal recoil-free fractions for all the phases.

Zeta potential of photocatalysts and dyes was measured in their aqueous solution in Zetasizer Nano-ZS of Malvern Company.

For characterization of the chemical surface structure of the photocatalyst FTIR/DR Spectroscopy was used. The spectra were recorded by means of JASCO FTIR 430 spectrometer with scanning speed of 50 scans/min and the resolution of 4 cm^{-1}. The background was taken before each measurement.

The content of carbon in the prepared samples was determined by combustion of carbon in air using TG analysis coupled with FTIR measurements. The samples were gradually heated up to 1000 °C in air with simultaneous recording of FTIR spectra of the decomposed gas products. The carbon content in the samples was calculated from the mass loss on the TG curve accompanied by appearing of CO$_2$ bands in the spectrum.

The analysis of OH radicals formation on the sample surface under UV irradiation with and without Fenton reagent (H$_2$O$_2$) was performed by fluorescence technique using coumarine, which readily reacts with OH radicals to produce highly fluorescent product, 7-hydroxycoumarine. The intensity of the peak attributed to 7-hydroxycoumarine is known to be proportional to the amount of OH radicals formed [23]. The product of coumarine hydroxylation, 7-hydroxycoumarine was determined by means of spectrofluorymeter Hitachi F-2500, the fluorescence spectra were recorded at excitation wavelength 332 nm for emission spectra in the range of 335–600 nm with λ$_{max}$ at around 460 nm.

2.3. Photocatalytic activity test

The photoactivities of prepared samples were tested for dyes decomposition (Methylene Blue (MB), Reactive Black (RB) and Acid Red (AR)), under UV irradiation with and without addition of H$_2$O$_2$. To check the influence of the light on the yield of photo-Fenton process some photocatalytic tests were performed in the dark (dark Fenton process) and under artificial visible light. The structures of dyes are presented in Fig. 1. Each time, for the photocatalytic test, the beaker with 500 ml of a dye solution of concentration around 0.03 g/L and 0.1 g of photocatalyst were used. The amount of H$_2$O$_2$ added to the solution was 9.8 mmol/L. The solutions were first magnetically stirred in a dark for 30 min in order to estimate the adsorption of dyes on the photocatalyst surface and then were irradiated under UV or visible lights from the top of the beaker. In dark Fenton process decomposition of dyes was carried out in the absence of any light with the preliminary adsorption for 30 min. The concentration of a dye solution was analyzed in UV–vis spectrophotometer, The Total Organic Carbon (TOC) was measured before and after decolourisation. As a source of UV, six lamps of Philips company with power of 20 W each were applied. These lamps emit the radiation at the visible region of about 100 W/m^2 and at UV range of 154 W/m^2 intensities, in the range of 312–553 nm with a maximum at around 350 nm. As a source of visible light the fluorescence lamps were used (4 × 18 W), which emit light in the visible region with intensity of 715 W/m^2 and insignificant amount of UV with intensity of 0.22 W/m^2.

3. Results

3.1. XRD measurements

XRD patterns of the original TiO$_2$ precursor and Fe-C-TiO$_2$ samples prepared by heating at different temperatures are shown in Fig. 2. After heating at 500 °C anatase phase in Fe-C-TiO$_2$ has been
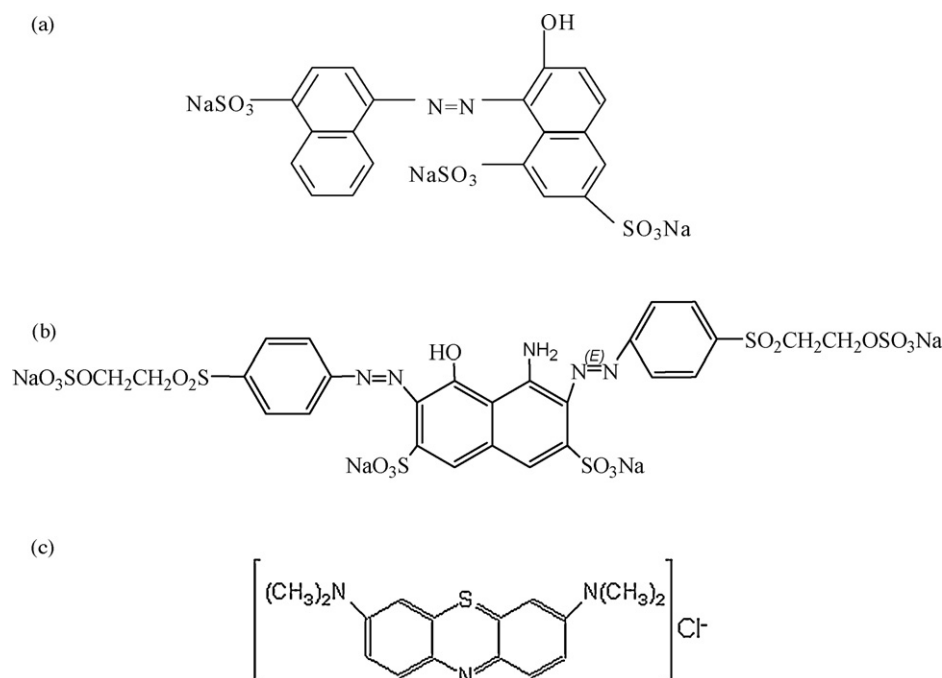
Fig. 1. The chemical structure of dyes, (a) Acid Red, (b) Reactive Black, and (c) Methylene Blue.

better crystallised, a small amount of rutile remained, and Fe_3O_4 with Fe_2O_3 (hematite), as the new phases were formed. At higher temperatures of heat-treatment, 600–800 °C, these phases were present in all the prepared samples, additionally anatase was transformed to rutile and $FeTiO_3$ phase appeared.

3.2. Mössbauer spectroscopy measurements

The Mössbauer spectra of the Fe-C-TiO_2 samples are shown in Fig. 3. The spectra represent the superposition of one or two doublets and one or three sextets. The Mössbauer parameters obtained from the numerical analysis are summarized in Table 1. Doublet I was attributed to the Fe(III) species probably ferric oxide Fe_2O_3 but in a paramagnetic form. The value of quadrupole splitting QS of this doublet, higher for samples A500 and A600 than usually expected for paramagnetic Fe_2O_3 (QS = 0.60–0.70 mm/s) may suggest the presence of this phase on the sample surface where the iron

ions have strongly disturbed symmetry. The parameters of Doublet II are characteristic for $FeTiO_3$ phase (ilmenite) which content depends on the temperature of heat treatment during the catalyst preparation. The higher temperature was applied, the higher content of this iron phase was observed. It is worthwhile to note that ilmenite was not found in the sample prepared at 500 °C.

Sextets I and II were assigned to magnetite and sextet III – to hematite. The latter phase dominated in sample prepared at 600 °C. The magnetic field of this hematite lower than the value of $H = 51.5$ T characteristic for bulk, well-crystallized material, suggested poor crystalline and small crystallites.

3.3. Content of carbon

It has been measured by TG-FTIR method that Fe-C-TiO_2 samples contained a residue carbon, which came from the carbonization of oxalate. In Table 2, the content of carbon and the conditions of heat treatment are listed. The highest content of carbon, 1.82 wt% was found in the sample prepared at 500 °C, the other samples contained less than 1 wt% of carbon. Lower content of carbon in the samples prepared at higher temperatures could be effected by a carbon oxidation through TiO_2 and its evolving during gas flow. Sample prepared at 600 °C has lower content of carbon than these prepared at 700 and 800 °C. It is suggested that more oxidative conditions at 600 °C conducted to carbon combustion, additionally can be noticed that these conditions resulted also in iron oxidation to Fe_2O_3 (this phase of iron was dominated only in the sample prepared at 600 °C).

3.4. Zeta potential

The values of measured the electrokinetic zeta potentials of the photocatalysts particles in the ultra pure water are listed in Table 2. Modification of TiO_2 caused reducing of zeta potential of anatase particles from +12.4 to −7 mV. Zeta potential of dyes used for decomposition are presented in Table 3. RB and AR are rather stable particles in the aqueous solution and have low values of
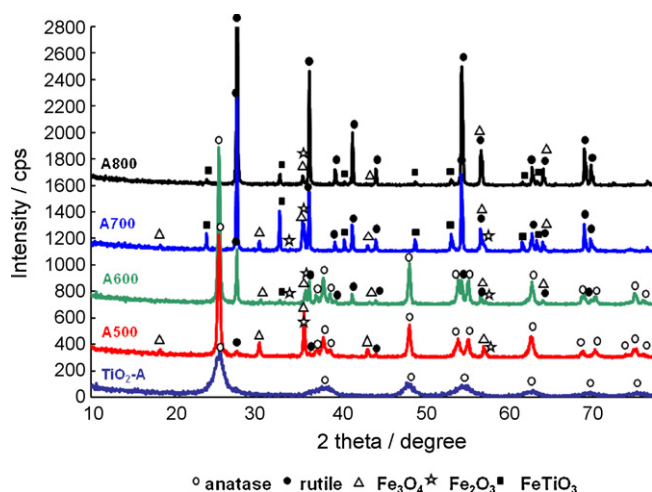

Fig. 2. XRD patterns of TiO_2 and prepared Fe-C-TiO_2 samples.
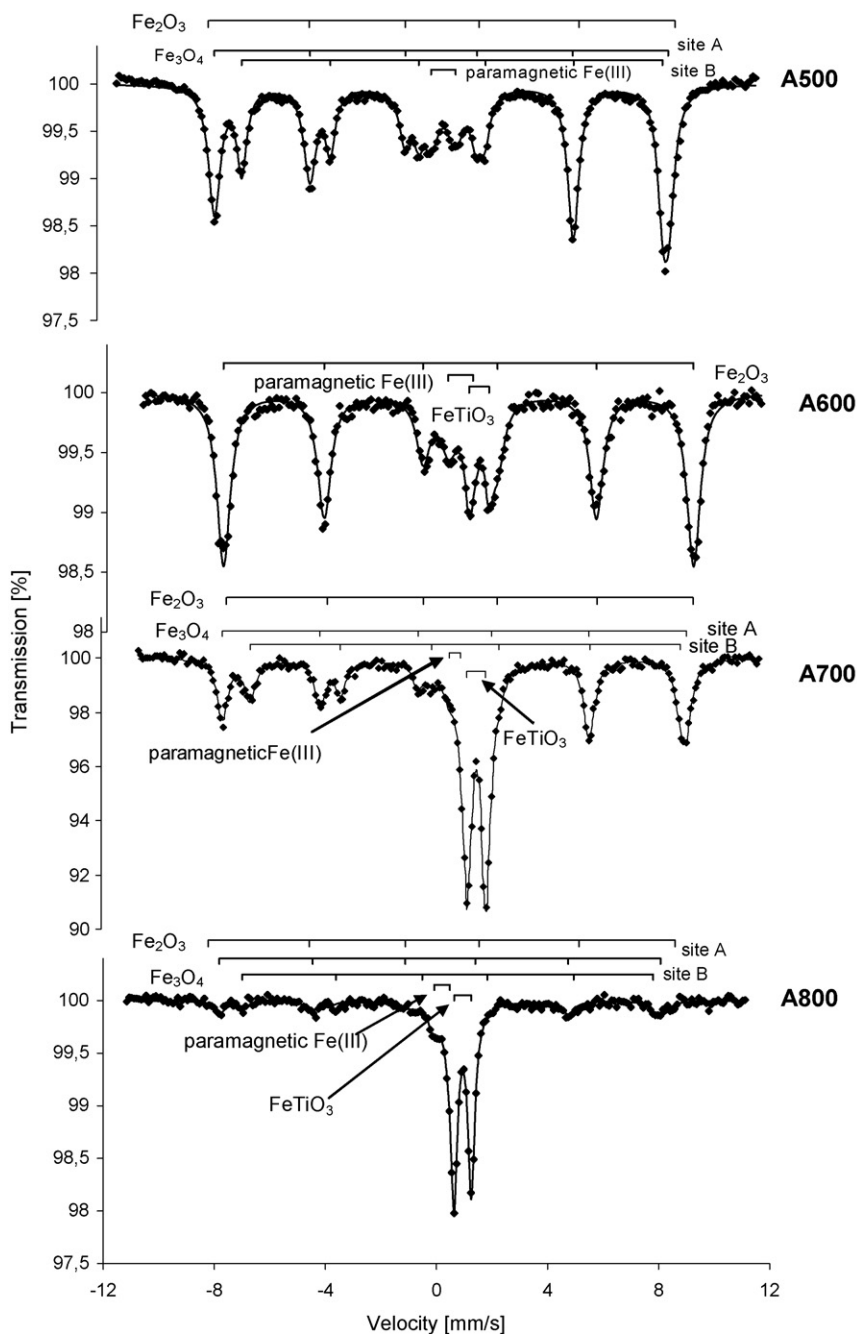
Fig. 3. Mössbauer spectra of the Fe-C-TiO$_2$ samples.

zeta potential, −46.8 and −37.9 mV, respectively, whereas MB particles are positively charged in the aqueous medium and their zeta potential is +4.3 mV.

3.5. FTIR measurements

FTIR spectra of the TiO$_2$ precursor and prepared Fe-C-TiO$_2$ samples are presented in Fig. 4. In the original TiO$_2$ some weakly marked bands could be observed: at the range of 3600–2600 cm^{-1} the broad band with a maximum at around 3300 cm^{-1} assigned for both, dissociated and molecularly adsorbed water, at 3695 cm^{-1} the band assigned to the hydroxyl groups chemisorbed on the surface defect side of the photocatalyst, and at 1623 cm^{-1} the band attributed to the molecular water [24]. In the modified samples

these bands have been reduced or completely disappeared due to the deposition of carbon. The sample prepared at 600 °C, which contained the lowest content of carbon showed the lowest reduction of hydroxyl groups, although at the same time some C=C groups were clearly observed. It is assumed that carbon deposition takes place on the site of hydroxyl groups. Reduction of hydroxyl groups on the surface of Fe-C-TiO$_2$ samples is a result of changes in the nature of photocatalyst surface from hydrophilic to hydrophobic.

3.6. OH radicals measurements

In Fig. 5, the formation of OH radicals on the photocatalyst surface during UV irradiation is presented. The increase of OH radicals formation with time of UV irradiation can be observed. The

Table 1
Mössbauer data for the Fe-C-TiO$_2$ samples prepared from anatase and rutile precursors

Mossbauer parameters		Sample			
		A500	A600	A700	A800
Doublet I paramagnetic iron Fe(III)	IS (mm/s)	0.37 (1)	0.38 (3)	0.30 (3)	0.31 (2)
	QS (mm/s)	0.86 (1)	0.84 (4)	0.40 (3)	0.57 (3)
	A (%)	13.1 (3)	13.2 ± 1.2	5.5 (5)	13.5 ± 1.0
Doublet II ilmenite (FeTiO$_3$)	IS (mm/s)	–	1.01 (1)	1.05 (1)	1.06 (1)
	QS (mm/s)	–	0.69 (2)	0.63 (1)	0.62 (1)
	A (%)	–	8.2 (8)	42.1 (6)	62.1 (8)
Sextet I magnetite Fe$_3$O$_4$ site A	IS (mm/s)	0.27 (1)	–	0.28 (1)	0.24 (3)
	H (kOe)	496.3 (5)	–	495.0 (8)	491 (2)
	A (%)	13.7 ± 4.5	–	11.5 ± 1.2	5.4 ± 1.2
Sextet II magnetite Fe$_3$O$_4$ site B	IS (mm/s)	0.68 (1)	–	0.65 (1)	0.56 (5)
	H (kOe)	463.3 (2)	–	461.6(6)	461(4)
	A (%)	31.4 (8)	–	23.0 ± 1.3	10.8 ± 2.5
Sextet III hematite Fe$_2$O$_3$	IS (mm/s)	0.33 (1)	0.33 (1)	0.33 (1)	0.35 (4)
	QS (mm/s)	0.02 (1)	0.06 (2)	0.02 (1)	0.02 (1)
	H (kOe)	503 (1)	506.9 (3)	504 (1)	510 (4)
	A (%)	41.8 ± 4.5	78.5 ± 4.3	17.9 ± 1.9	8.1 ± 3.4

IS – isomer shift versus room temperature α-Fe, QS – quadrupole splitting, A – relative contribution to the total spectrum, H – magnetic field.

Table 2
Zeta potentials of photocatalysts and carbon content in the prepared Fe-C-TiO$_2$ samples

| Sample	HTT (°C)	Zeta potential, ξ (mV)	Carbon content (wt%)
TiO$_2$-A	–	12.4	–
A500	500	2.3	1.82
A600	600	3.4	0.23
A700	700	3.3	0.70
A800	800	−7	0.38

Table 3
The chemical structures and zeta potentials of dyes

Dye	Molecular weight (g/mol)	Zeta potential, ξ (mV)
Acid Red	604.5	−39.7
Reactive Black	991.8	−46.8
Methylene Blue	319.9	+4.3

Fe-C-TiO$_2$ samples showed lower amount of OH radicals formation than the original TiO$_2$. Deposition of carbon on the site of hydroxyl groups could cause decreasing the yield of OH radicals formation, which are mainly generated by the reaction of photoinduced holes in semiconductor with the adsorbed molecular water on its surface.
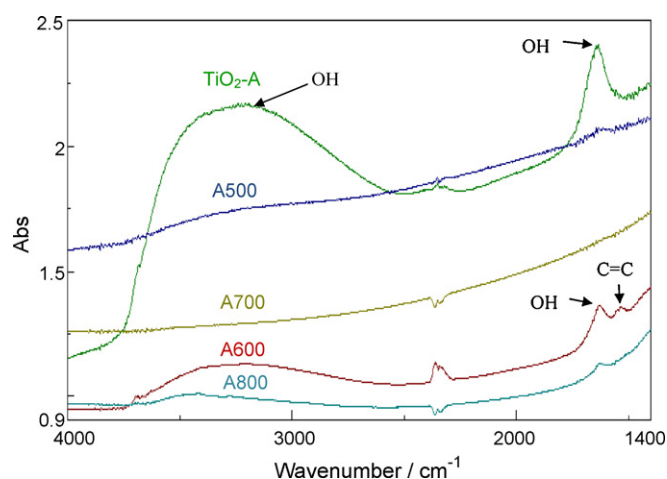
Fig. 4. FTIR spectra of TiO$_2$ and prepared Fe-C-TiO$_2$ samples.
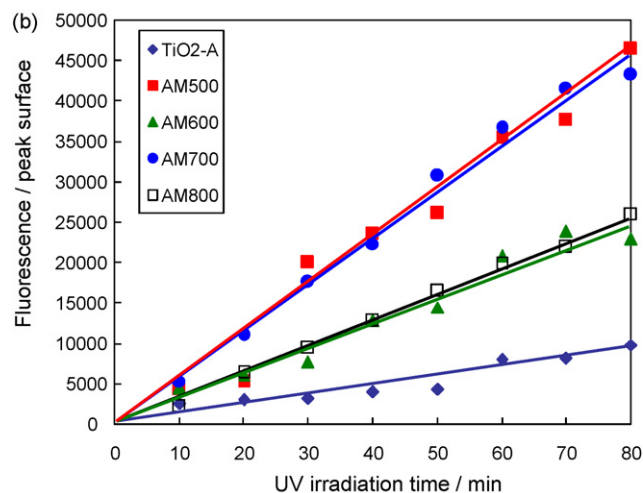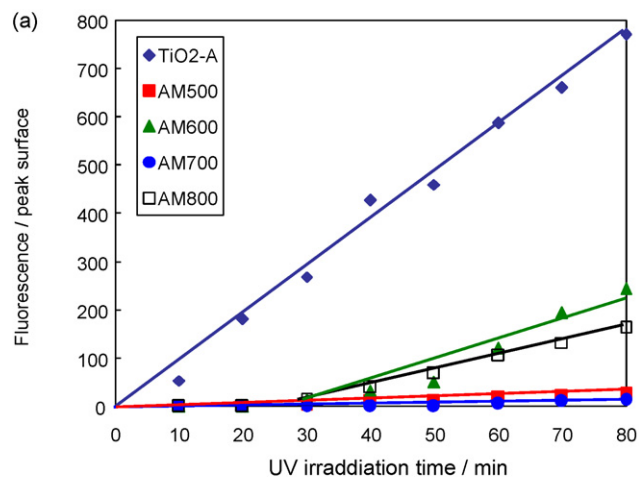
Fig. 5. Formation of OH radicals on the photocatalysts surface, (a) under UV radiation, (b) under UV radiation with addition of H$_2$O$_2$.
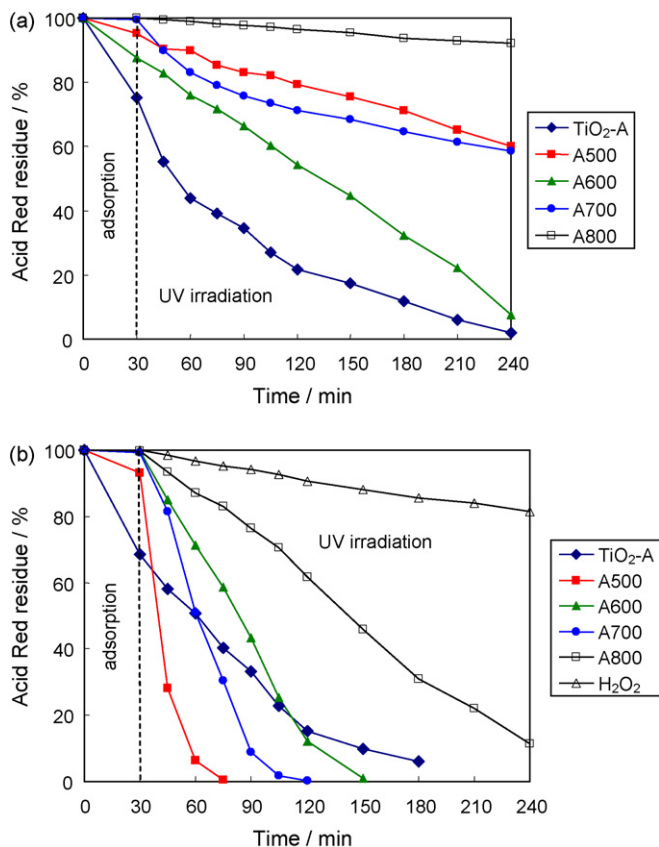
Fig. 6. Acid Red decomposition on TiO$_2$ and prepared Fe-C-TiO$_2$ samples, (a) under UV radiation, (b) under UV radiation with addition of H$_2$O$_2$.

The higher deposition of carbon in Fe-C-TiO$_2$ samples the lower rate of OH radicals formation is observed with time of UV irradiation.

After addition of H$_2$O$_2$ to the reaction solutions, Fe-C-TiO$_2$ photocatalysts indicated significant increase of the OH radicals formation, what was certainly caused by an iron oxidation in photo-Fenton reaction. The differences in the amount of OH radicals formation upon the UV irradiation on Fe-C-TiO$_2$ samples in the presence of H$_2$O$_2$ were caused by the different activity of the iron phases. Fe-C-TiO$_2$ samples, which showed higher rate of OH radicals formation than the other samples consisted from higher amount of magnetite.

3.7. Adsorption and decomposition of dyes under UV irradiation

Decomposition of AR on TiO$_2$ and Fe-C-TiO$_2$ samples under UV irradiation only and under UV with addition of H$_2$O$_2$ is shown in Fig. 6. The anatase type TiO$_2$ indicated higher adsorption of AR on its surface than prepared Fe-C-TiO$_2$ samples and also higher rate of AR decomposition. TiO$_2$ itself decomposed AR in 98% after 30 min adsorption and 210 min of UV irradiation, whereas Fe-C-TiO$_2$ prepared at 600 °C decomposed AR at the same time in 92%. The other samples showed much slower decomposition rate than the original TiO$_2$. Addition of H$_2$O$_2$ to the reaction mixture accelerated AR decomposition on all Fe-C-TiO$_2$ samples. The highest rate of reaction was observed on A500 sample which revealed nonlinear character of decomposition. Similar tendency, but with lower reaction rate, can be seen for A700 and A600 samples. The decomposition of AR on A800 seems to be linear and much slower. The Total Organic Carbon (TOC) measured before and after decolourization showed mineralisation degree in the range of 42–50%, so some byproducts of AR degradation remained in the solution.
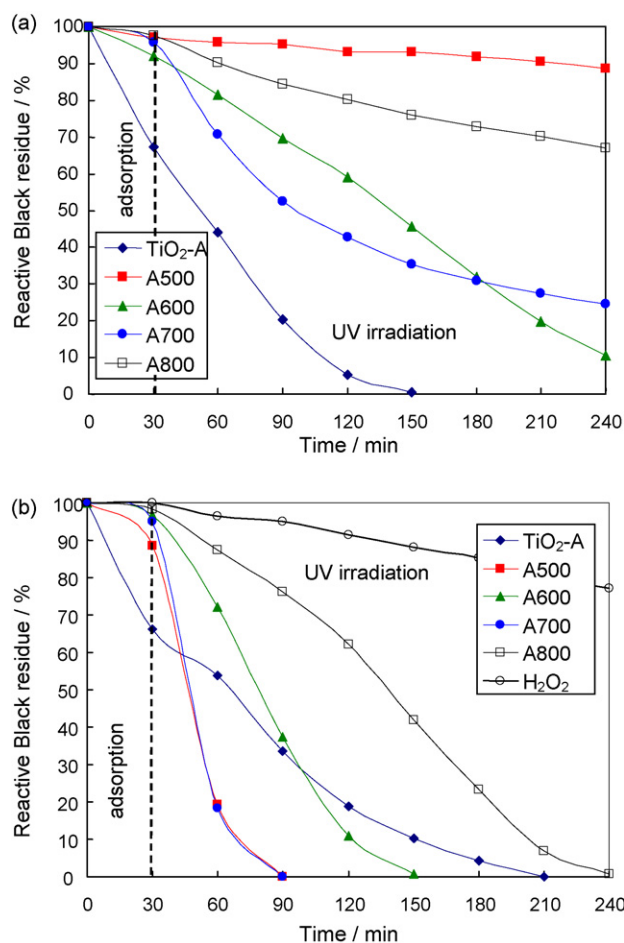

Fig. 7. Reactive Black decomposition on TiO$_2$ and prepared Fe-C-TiO$_2$ samples, (a) under UV radiation, (b) under UV radiation with addition of H$_2$O$_2$.

Decomposition of RB on TiO$_2$ and Fe-C-TiO$_2$ is shown in Fig. 7. Similar behaviour of RB adsorption and decomposition was observed as it was in case of AR solution, anatase type TiO$_2$ exhibited high adsorption of RB and high degree of decomposition under UV irradiation, however, this decomposition rate was much slower than on Fe-C-TiO$_2$ when H$_2$O$_2$ was added to the RB solution. A500 and A700 samples decomposed RB under UV with H$_2$O$_2$ within 60 min of UV irradiation whereas with TiO$_2$ photocatalyst this process took place 180 min. Hydrogen peroxide itself was not efficient for RB decomposition, only 20% of dye was decomposed after 210 min of UV irradiation.

Decomposition of MB on TiO$_2$ and Fe-C-TiO$_2$ is shown in Fig. 8. It can be observed that MB is poorly adsorbed on all the tested photocatalysts, and its decomposition under UV irradiation is going slowly. Anatase type TiO$_2$ appeared to be the most active in comparison with prepared Fe-C-TiO$_2$ photocatalysts. Addition of H$_2$O$_2$ to the MB solution caused significant acceleration of MB decomposition on Fe-C-TiO$_2$ samples, however, this decomposition rate was much slower than in case of azo dyes decomposition: AR and RB. Hydrogen peroxide was also not efficient in MB decomposition.

To summarise decomposition of dyes on TiO$_2$ and Fe-TiO$_2$ photocatalysts it has to be pointed out that photo-Fenton reaction occurring on Fe-C-TiO$_2$ samples gives high amount of OH radicals formation and significantly accelerates decomposition of dyes, especially azo dyes: AR and RB. A500 sample was the most active in dyes decomposition, however, A700 sample prepared at 700 °C showed also high photoactivity, especially for RB decomposition.
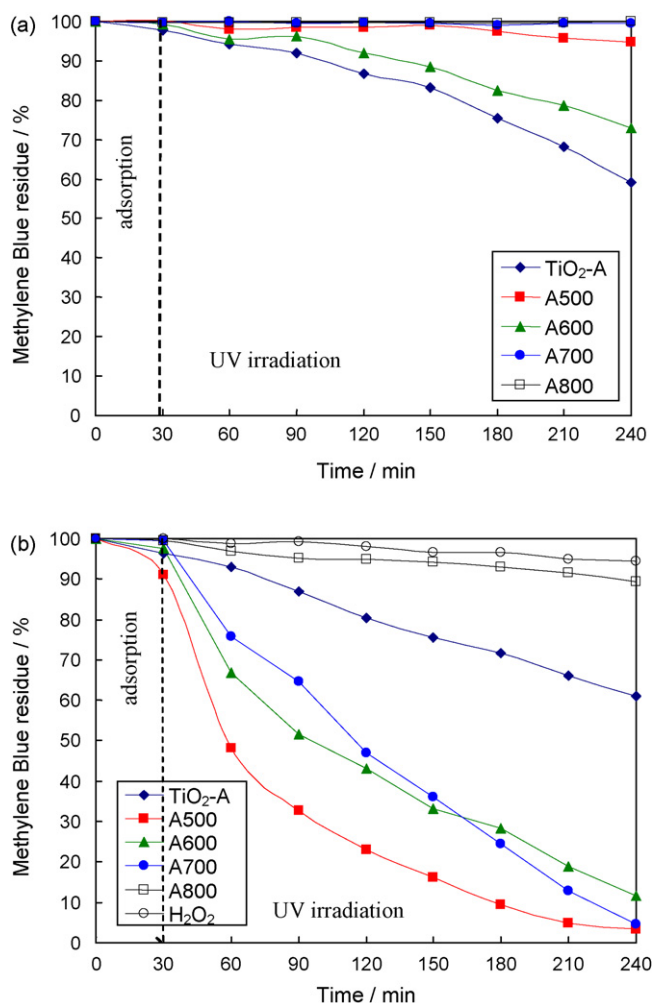
Fig. 8. Methylene Blue decomposition on TiO$_2$ and prepared Fe-C-TiO$_2$ samples, (a) under UV radiation, (b) under UV radiation with addition of H$_2$O$_2$.

Adsorption of dyes on the photocatalysts surface supports their decomposition under UV irradiation, however, high quantity of generated OH radicals is the most effective factor in the mineralisation of dyes. AR and RB are going decomposition through OH radicals much easier than MB. Both azo dyes are anionic in the aqueous solutions, and they favored adsorb on the positively charged surface, therefore high adsorption of AR and RB was observed on unmodified TiO$_2$, which influenced its high photoactivity. These results are consent with those reported by other authors, who proved that adsorption of RB 5 was favored on the positively charged surface [25]. MB with positive zeta potential was not quantatively adsorbed either on TiO$_2$ or Fe-C-TiO$_2$ photocatalysts, therefore, was decomposed slower than the other azo dyes. Improving decomposition of MB through increasing its adsorption on the photocatalyst surface, especially on carbon/TiO$_2$ was widely reported in the literature [26,27].

In case of azo dyes, AR and RB the dual hole-radical mechanism of decomposition probably occurs, because high adsorption of these dyes on the surface of TiO$_2$ resulted in their high decomposition rate, higher than on the prepared Fe-C-TiO$_2$ photocatalysts, however, significant increase of OH radicals formation on the prepared samples in the presence of H$_2$O$_2$ resulted in high acceleration of dyes decompositions.

The dual mechanism of RB 5 decomposition on different semiconductors was described by Poulios and Tsachpinis [28], according

to this mechanism direct h$^+$ oxidation of the ethyl-sulfuric and sulfuric groups take place in combination with the OH attack of the benzene and naphthalene rings. Positively charged TiO$_2$ offers a suitable surface for adsorption of RB5 from the ethylsulfonic group. This bond has a relatively high covalent character, and the oxygen atoms of the group, being relatively strong electron donors, are able to directly interact with valence band holes, thus facilitating direct electron transfer. The increased distance between the reactants no longer allows direct charge transfer, resulting in the reduction of the reaction state [28]. The reductive pathway has also been proposed by several authors for the degradation of azo dyes [29,30]. According to this model, transfer of a photogenerated electron from the conduction band of TiO$_2$ to the dye molecule takes place, thus leading to the reduction of the azo linkage and consequently to the decolourisation of the solution, the OH radicals attack also occurs.

The radical mechanism of AR decomposition via photo-Fenton process was also reported in the literature [31], which was explained due to the Fe^{3+} photocatalyzed reactions, i.e. photolysis of hydroxide complexes of Fe^{3+} yielding hydroxyl radicals and regenerating Fe^{2+} and photochemical reactions of complexes formed between Fe^{3+} and the organic substrate or its degradation intermediates, especially organic acids. High efficiency of AR decomposition was observed in the presence of ferrioxalate, because of its high molar absorption coefficient for longer wavelengths and generation of hydroxyl radicals with a high quantum yield [31].

3.8. Adsorption and decomposition of Reactive Black in a dark Fenton and photo-assisted Fenton processes

Comparison of Fenton and photo assisted Fenton processes was done by testing decomposition of RB on the Fe-C-TiO$_2$ sample prepared at 700 °C. Detection of OH radicals in formed dark Fenton and photo supported Fenton processes was performed. In Fig. 9, decomposition of RB under UV, vis and in a dark on TiO$_2$ and A700 samples is shown together with generation of OH radicals in these processes. It can be observed low decomposition rate of RB with H$_2$O$_2$ used under UV irradiation. It was reported in the literature that amount of OH generated directly by the photolysis of H$_2$O$_2$ under UV-A is very small [32]. H$_2$O$_2$ does not absorb at all the light with the wavelength above ∼320 nm. Almost no decomposition of dye was observed in a dark Fenton process, the measured amount of OH radicals formation in this process was also insignificant in comparison with vis or UV irradiation. Fe-C-TiO$_2$ photocatalyst prepared at 700 °C showed photoactivity in photo-Fenton process under visible light irradiation, its photoactivity was comparable with that of TiO$_2$ irradiated with UV light, however, lower than in case when UV was applied. The other researchers investigated decomposition of RB 5 (RB5) on the alumina supported iron oxide composites and they reported that the presence of UV-A light effectively promotes mineralisation of RB 5 [32]. They also pointed out that positively charged surface of photocatalyst favors the adsorption of anionic azo dye RB 5 [32]. TiO$_2$ particles were more positively charged than the other prepared Fe-C-TiO$_2$ samples, what could explain the result of high adsorption of RB on their surface, which undoubtedly supported their activity towards dye decomposition.

Poor efficiency of dark Fenton can be explain by the insignificant amount of OH radicals formation and oxidation of Fe^{3+} ions to Fe(HO$_2$)$^{2+}$, yielding in HOO$^•$ radicals reaction (3) and (4) which cannot effectively mineralise RB5:

$$Fe^{3+} + H_2O_2 \rightarrow Fe(HO_2)^{2+} \tag{3}$$

$$Fe(HO_2)^{2+} \rightarrow Fe^{2+} + HO_2^{•} \tag{4}$$
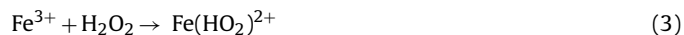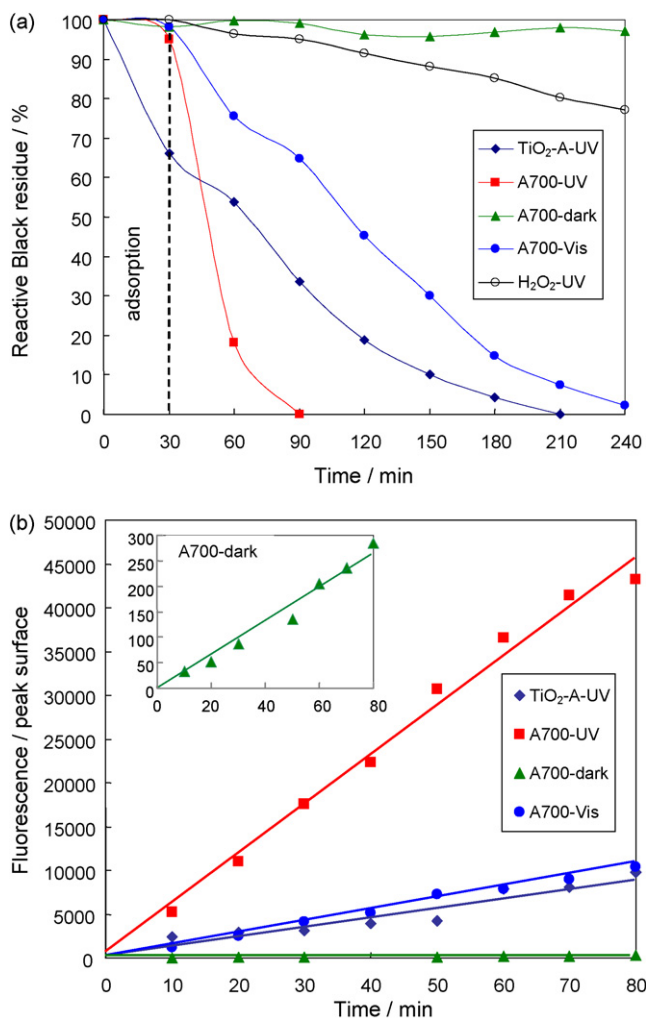
Fig. 9. (a) Decomposition of Reactive Black on TiO_2 and A700 samples in Fenton and photo-Fenton processes (in dark, under UV and visible lights), and (b) formation of OH radicals in these processes.

$OH^\bullet$ radicals can be quantitatively produced in the presence of light, according to reaction (5):

$$Fe(HO_2)^{2+} + h\nu \rightarrow Fe^{2+} + HO^\bullet \tag{5}$$

$Fe(HO_2)^{2+}$ ion absorbs light at wavelengths up to about 410 nm, therefore producing of $HO^\bullet$ radicals in reaction (5) is possible under both, UV and visible lights, however, with UV light this reaction is more efficient. The above considerations can explain the photocatalytic activity of A700 sample under UV, vis, and in a dark Fenton processes.

4. Conclusions

Modification of TiO_2 by the carbon and iron changed the nature of photocatalyst from hydrophilic to hydrophobic and therefore decrease of OH radicals formation on the surface of prepared photocatalysts was observed. However, formation of OH radicals on Fe-C-TiO_2 surface under UV increased extensively after addition of H_2O_2, due to the iron oxidation and the photo-Fenton reactions occurring. Fenton process without any light was not effective for dye degradation. Both, UV and visible lights supported the yield of Fenton reactions, however, the former was more efficient, because resulted in higher quantum yield of hydroxyl radicals than the latter. These hydroxyl radicals took part in the dyes decomposi-

tions. The dual hole-radical mechanism for dyes decomposition was observed. According to this mechanism, the direct oxidation of holes with adsorbed molecules of dyes occurs in combination with OH radicals attack. The azo dyes, AR and RB of anionic character in the aqueous solutions were adsorbed on the positively charged surface of the photocatalysts in higher quantity than MB, which has positive zeta potential in the solution, and therefore they proceeded degradation much faster than MB. The photolysis of H_2O_2 under applied UV irradiation was insignificant and did not promote the dyes decomposition.

In general, Fe-C-TiO_2 samples, which contained higher amount of a residue carbon(A500 and A700) showed higher amount of OH radicals formation under UV with H_2O_2 than the original TiO_2 and those with low content of carbon. The samples with higher content of a residue carbon had some iron phases like Fe_3O_4 or Fe_2O_3 on their surface, which were not built in TiO_2 lattice. It was observed that the presence of paramagnetic iron and Fe_3O_4 can enhance the photocatalytic activity of Fe-C-TiO_2 photocatalysts in photo-Fenton process with applied UV and H_2O_2, whereas $FeTiO_3$ phase is poorly active. Therefore, lower temperature of Fe-C-TiO_2 preparation like $500\,^\circ C$ is more favored for preparation of photocatalysts active in photo-Fenton process.

Acknowledgement

References

[1] E. Piera, M.I. Tejedor, M.E. Zorn, M.A. Anderson, Degradation of chlorophenols by means of advanced oxidation processes: a general review, Appl. Catal. B: Environ. 47 (2004) 219–256.

[2] A. Fujishima, K. Hashimoto, T. Watanabe, TiO2 Photocatalysis Fundaments and Applications, published by BKC, Inc., May 1999.

[3] C.G. Silva, W. Wang, J.L. Faria, Photocatalytic and photochemical degradation of mono-, di- and tri-azo dyes in aqueous solution under UV irradiation, J. Photochem. Photobiol. A: Chem. 181 (2006) 314–324.

[4] V. Shah, P. Verma, P. Stopka, J. Gabriel, P. Baldrian, F. Nerud, Decolorization of dyes with copper (II)/organic acid/hydrogen peroxide systems, Appl. Catal. B: Environ. 46 (2003) 287–292.

[5] I.K. Konstantinou, T.A. Albanis, Photocatalytic transformation of pesticides in aqueous titanium dioxide suspensions using artificial and solar light: intermediates and degradation pathways, Appl. Catal. B: Environ. 42 (2003) 319–335.

[6] T. Sauer, G. Cesconeto Neto, H.J. Jose, R.F.P.M. Moreira, Kinetics of photocatalytic degradation of reactive dyes in a TiO2 slurry reactor, J. Photochem. Photobiol. A: Chem. 149 (2002) 147–154.

[7] C. Wang, C. Bottcher, D.W. Bahnemann, J.K. Dohrmann, A comparative study of nanometer sized Fe(III)-doped TiO2 photocatalysts: synthesis, characterization and activity, J. Mater. Chem. 13 (2003) 2322–2329.

[8] S. Nahar, K. Hasegawa, S. Kagaya, Photocatalytic degradation of phenol by visible light-responsive iron-doped TiO2 and spontaneous sedimentation of the TiO2 particles, Chemosphere 65 (2006) 1976–1982.

[9] J. Arana, O. Gonzalez Diaz, M. Miranda Saracho, J.M. Dona Rodriguez, J.A. Herrera Melian, J. Perez Pena, Photocatalytic degradation of formic acid using Fe/TiO2 catalysts: the role of Fe3+/Fe2+ ions in the degradation mechanism, Appl. Catal. B: Environ. 32 (2001) 49–61.

[10] C. Wang, D.W. Bahnemann, J.K. Dohrmann, A novel preparation of iron-doped TiO2 nanoparticles with enhanced photocatalytic activity, Chem. Commun. 16 (2000) 1539–1540.

[11] J.A. Navio, G. Colon, M. Macias, C. Real, M.I. Litter, Iron-doped titania semiconductor powders prepared by a sol–gel method. Part I. Synthesis and characterization, Appl. Catal. A: Gen. 177 (1999) 111–120.

[12] J.A. Navio, J.J. Testa, P. Djedjeian, J.R. Padron, D. Rodriguez, M.I. Litter, Iron-doped titania powders prepared by a sol–gel method. Part II. Photocatalytic properties, Appl. Catal. A: Gen. 178 (1999) 191–203.

[13] J. Arana, O. Gonzalez Diaz, J.M. Dona Rodriguez, J.A. Herrera Melian, C. Garriga i Cabo, J. Perez Pena, M. Carmen Hidalgo, J.A. Navio-Santos, Role of Fe3+/Fe2+ as TiO2 dopant ions in photocatalytic degradation of carboxylic acids, J. Mol. Catal. A: Chem. 197 (2003) 157–171.

[14] X.-H. Qi, Z.-H. Wang, Y.-Y. Zhuang, Y. Yu, J.-L. Li, Study on the photocatalysis performance and degradation kinetics of X-3B over modified titanium dioxide, J. Hazard. Mater. B118 (2005) 219–225.

[15] C. Karunakaran, S. Senthilvelan, Fe2O3-photocatalysis with sunlight and UV light: oxidation of aniline, Electrochem. Commun. 8 (2006) 95–101.

[16] L. Zhang, P. Li, Z. Gong, A. Oni, Photochemical behavior of benzo[a]pyrene on soil surfaces under UV light irradiation, J. Environ. Sci. 18 (2006) 1226–1232.

[17] M. Sadeghi, W. Liu, T.-G. Zhang, P. Stavropoulos, B. Levy, Role of photoinduced charge carrier separation distance in heterogeneous photocatalysis: oxidative degradation of CH_3OH vapor in contact with Pt/TiO_2 and cofumed TiO_2-Fe_2O_3, J. Phys. Chem. 100 (1996) 19466–19474.

[18] J.C. Crittenden, J. Liu, D. Hand, D. Perram, Photocatalytic oxidation of chlorinated hydrocarbons in water, Water Res. 31 (1997) 429–438.

[19] B. Tryba, M. Toyoda, A.W. Morawski, M. Inagaki, Modification of carbon-coated TiO_2 by iron to increase adsorptivity and photoactivity for phenol, Chemosphere 60 (2005) 477–484.

[20] B. Tryba, A.W. Morawski, M. Inagaki, M. Toyoda, The kinetics of phenol decomposition under UV irradiation with and without H_2O_2 on TiO_2, Fe-TiO_2 and Fe-C-TiO_2 photocatalysts, Appl. Catal. B: Environ. 63 (2006) 215–221.

[21] B. Tryba, A.W. Morawski, M. Inagaki, M. Toyoda, Effect of the carbon coating in Fe-C-TiO_2 photocatalyst on phenol decomposition under UV irradiation via photo-Fenton process, Chemosphere 64 (2006) 1225–1232.

[22] B. Tryba, M. Inagaki, M. Toyoda, A.W. Morawski, Effect of TiO_2 precursor on the photoactivity of Fe-C-TiO_2 photocatalysts for Acid Red (AR) decomposition, J. Adv. Oxidation Technnol. 10 (2007) 267–272.

[23] K. Ishibashi, A. Fujishima, T. Watanabe, K. Hashimoto, Detection of active species in TiO_2 photocatalysis using the fluorescence technique, Electrochem. Commun. 2 (2000) 207–210.

[24] M. Kaneko, I. Okura, Photocatalysis Science and Technology, Springer, Kodansha, 2002, 117.

[25] M. Muruganandham, N. Sobana, M. Swaminathan, Solar assisted photocatalytic and photochemical degradation of Reactive Black 5, J. Hazard. Mater. B137 (2006) 1371–1376.

[26] T. Tsumura, N. Kojitani, I. Izumi, N. Iwashita, M. Toyoda, M. Inagaki, Carbon coating of anatase-type TiO_2 and photoactivity, J. Mater. Chem. 12 (2002) 1391–1396.

[27] B. Tryba, A.W. Morawski, T. Tsumura, M. Toyoda, M. Inagaki, Hybridization of adsorptivity with photocatalytic activity – carbon-coated anatase, J. Photochem. Photobiol. A: Chem. 167 (2004) 127–135.

[28] I. Poulios, I. Tsachpinis, Photodegradation of textile dye Reactive Black 5 in the presence of semiconducting oxides, J. Chem. Technnol. Biotechnol. 74 (1999) 349–357.

[29] K. Huster, Photocatalytic degradation of selected azo dyes, Chemosphere 24 (1992) 335–342.

[30] W. Tang, H. An, UV/TiO_2 photocatalytic oxidation of commercial dyes in aqueous solutions, Chemosphere 31 (1995) 4157–4170.

[31] J.R. Dominguez, J. Beltran, O. Rodriguez, Vis and UV photocatalytic detoxification methods (using TiO_2, TiO_2/H_2O_2, and $Fe^{3+}/H_2O_2/C_2O_4^{2-}$) for dyes treatment, Catal. Today 101 (2005) 389–395.

[32] C.L. Hsueh, Y.H. Huang, C.Y. Chen, Novel activated alumina-supported iron oxide-composite as a heterogeneous catalyst for photooxidative degradation of reactive black 5, J. Hazard. Mater. B129 (2006) 228–233.